

Electrochemical Applications

1/2002

Advances in electrochemical applications of impedance spectroscopy
 Issued and © by ZAHNER-elektrik GmbH & Co. KG in June 2002

First of all ...

... we have to say sorry for the long time you had to wait for this new issue of *Electrochemical Applications*. The delay was mainly caused by two facts: on the one hand we developed a lot of new products like the high current potentiostats of the EL- and the PP-series, the NOISE probe with outstanding features (not only for noise measurements) and the new PC interface which is running under Windows95/98 as well as under WindowsNT/2000 now. On the other hand we had a lot of scientific presentations at well-known meetings which yield enough stuff for the next issues of *Electrochemical Applications*.

Due to these facts we increased the Zahner team, and I am proud to introduce to you Dr. Werner Strunz, our new co-worker. He studied chemistry in Heidelberg, Germany and took his doctor's degree on "Electrical Conducting Coordination Polymers". He is supporting the Zahner team in several software projects and – above all – he is enhancing our scientific

work. You will find him as a co-author of various scientific presentations.

The recent issue of *Electrochemical Applications* does focus not only on EIS but on associated methods which are able to complement EIS in specific applications. First of all, there is the HCl (**H**igh **C**urrent **I**nterrupt) method, which allows you to find results in low impedance objects such as power generating devices even at high frequencies. The relaxation voltammetry is an alternative method for investigating high impedance systems such as coatings. The EIS chapter of this issue comes from Dr. Hoffmann (MTU-Friedrichshafen GmbH) who is demonstrating the application of *AC impedance spectroscopy on molten carbonate fuel cells*.

We hope, the topics of this issue are a good excuse for the long waiting period.
 Your Zahner Team

Current Interrupt Technique - Measuring low impedances at high frequencies

F. Richter, Siemens AG, KWU, Erlangen, Germany,
 franz.richter@erl11.siemens.de

C.-A. Schiller, Zahner-elektrik, Kronach, Germany,
 cas@zahner.de

N. Wagner, DLR, Stuttgart, Germany,
 norbert.wagner@dlr.de

If a power generating device is examined, its dynamic electrical equivalence generally will appear as a network which represents anode, cathode, membrane, electrolyte, and connectors.

The specific losses of every partial impedance of the network contribute to the overall efficiency of the device. The porous layers of anode and cathode, responsible for the charge transfer reaction, normally play a major role. Other contributions seem to be much less important. There is the resistance of the electrolyte or the membrane as well as the resistance of contacts and connectors. A dynamic part is added by the inductance of the body and the connectors.

Nevertheless, the ohmic part (electrolyte, membrane, connectors) plays an important role regarding the

performance of the device and accounts sometimes for the main part of the overall losses. It is very sensitive to degradation caused by corrosion and thermal stress.

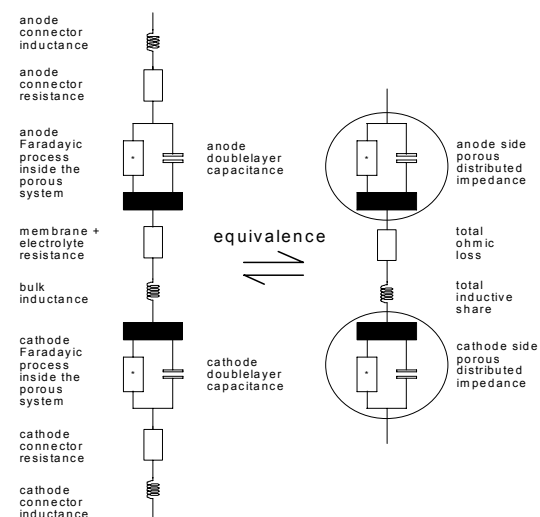


Fig. 1: Simplified electrical equivalent circuit of a typical electrochemical power source device

In applications with dynamic load changes the inductive parts, for example in a laptop computer battery or in electromotive applications, are limiting the maximum pulse load available.

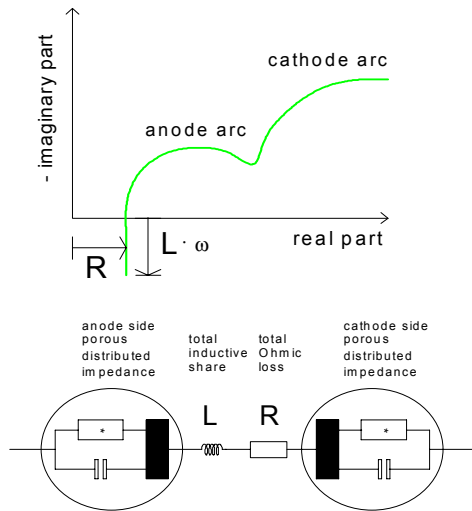


Fig. 2: The appearance of ohmic share and stray inductance in a fuel cell spectrum

EIS allows to separate all contributions and to determine the ohmic part in the high frequency region of a spectrum, where the impedance curve intersects the real axis. The inductance is shown at successive higher frequencies in the diagram. But there is one great restriction: Measuring impedance always means to measure two signals, current and voltage.

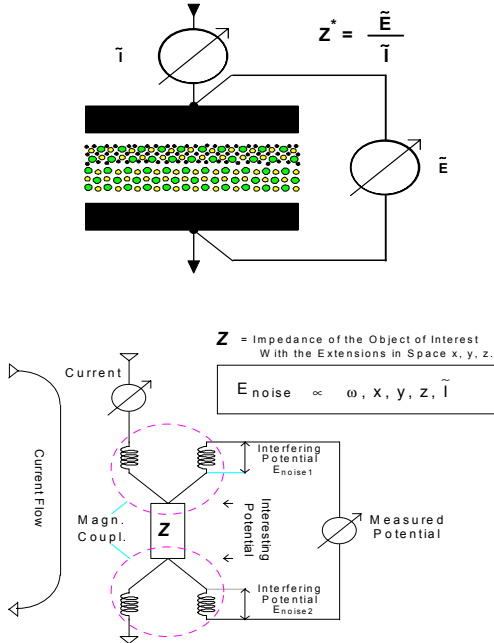


Fig. 3: Basic impedance measurement circuit – principle (top) and detail (bottom)

A closer look at the circuit in figure 3 shows that the potential information does not only contain the interesting part from the site of the connecting terminals.

It is rather contaminated by dynamically induced error voltages. These errors are caused by unavoidable mutual induction from the magnetic field of the current circuit.

The interference increases with increasing frequency and with the strength of the magnetic field of the current. It depends on the geometry and grows with the dimensions of the object. For the investigation of power sources this means: The more you scale up, the lower is the available upper frequency limit (f_g). Finally, there is a limit for the EIS at low ohmic objects. At a rough estimation you can calculate with:

$$f_g \approx 1 \text{ MHz} * |Z|_{\min} / \text{Ohm}$$

As a consequence, the window for getting an Ohmic resistance information by means of the EIS gets smaller for bigger cells. For certain systems, the window will be closed.

What can be done to complement the EIS under these conditions? The question is answered by the well known current interrupt technique, which does not need the knowledge of two signals simultaneously. The principle is depicted in figure 4 and explained in the following:

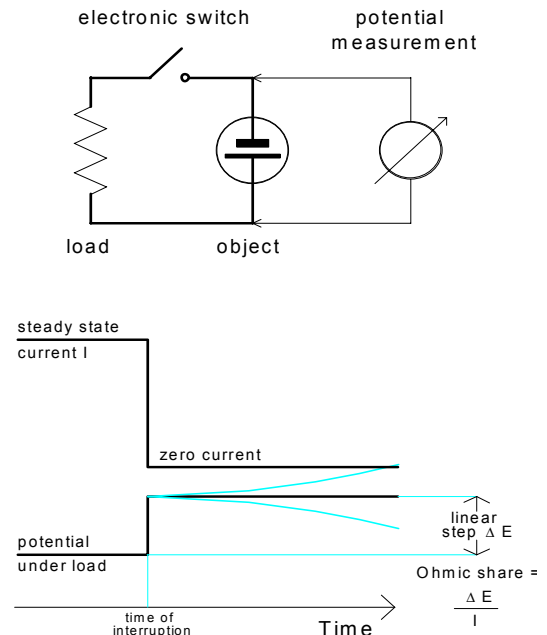


Fig. 4: Principle of current interrupt technique to determine the ohmic share

A steady-state current is interrupted by a switch. The step response of the potential is sampled and analysed assuming that the current drops instantaneously from its stationary value to zero.

In practice, the settling time depends on the electromagnetic energy stored in the parasitic capacity and inductivity of the cell arrangement on the one hand and the damping process on the other hand.

Provided that the set-up is built appropriate, the interruption results in a breakdown of the current to at least small values within a short time. In this case, the potential will be disturbed much less by mutual induction compared with an EIS measurement.

In theory, the ohmic contribution to the overall impedance can be easily seen from the height of the fast rectangular step of the potential. For the evaluation a linear step model is commonly used.

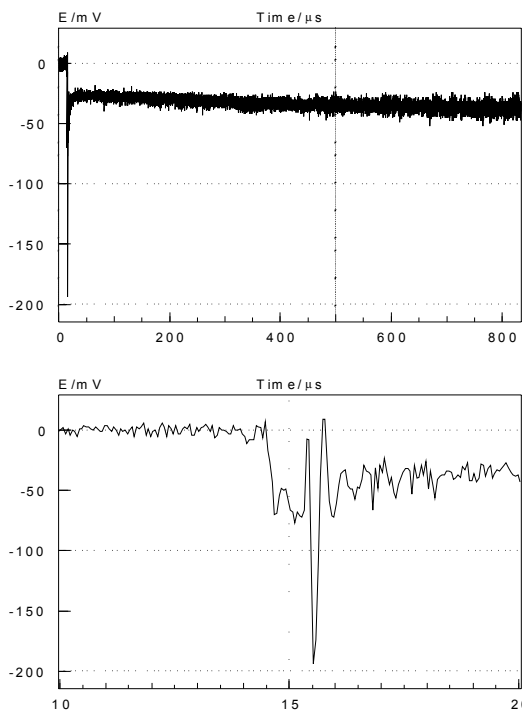
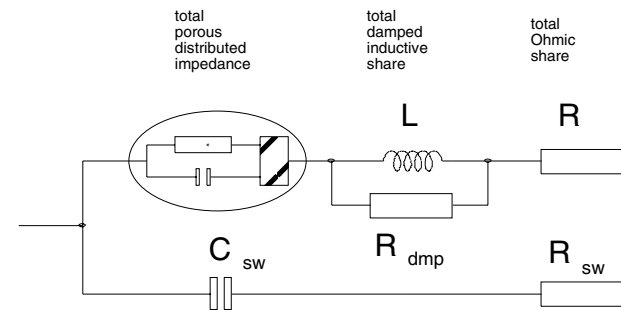


Fig. 5: Typical current interrupt potential step response. Long (top) and short (bottom) term response of a single cell PEM fuel cell at 80 A.

But this evaluation suffers from the fact that the analysis of the time domain data is interfered by the “ringing” in the signal as a result of the parasitic resonance. In addition, the early phase of the response is characterized by a non-linear behavior due to the imperfect characteristics of the electronic switch. Furthermore, the response of both double-layers may follow soon after the interruption when the concentrations of the involved species turn from their steady state values to new ones without load. All these effects bend and distort the expected ideal shape of the potential step. Therefore, the automatic analysis of pulse measurements by means of a simple fit to a linear step model often leads to inaccurate results.

Our aim was to improve the method in order to get results of comparable reliability to the EIS. The basic idea is not to evaluate the distorted step function in the time domain. Instead, after a transformation of the data into the frequency domain, the resulting

spectrum and all parasitic effects can be analysed by means of EIS methods.



$C_{sw}R_{sw}$: Capacitance and resistance of the electronic switch.
 R_{dmp} : Damping of the inductive share due to spatial distribution.

Fig. 6: Approximate equivalent circuit for a complete high current interrupt measurement set-up of an electrochemical power source device.

In figure 6, a simplified equivalent circuit for a complete HCI measurement set-up of a power cell is shown. It contains the impedance of the active cell part (circle), the integral inductance (L) and resistance (R) and the parasitic effects of the switch circuit. The resonance circuit is mainly built of the series inductance, the double layer capacity and the capacity of the electronic switch. It is responsible for the overshoot and “ringing” in the pulse response signal.

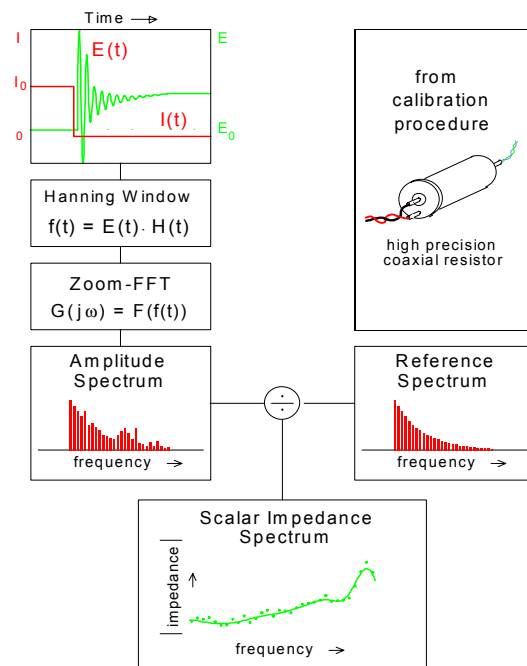


Fig. 7: Principle scheme of the Zahner high current interrupt data processing.

Figure 7 illustrates the essential steps for the transformation of the time domain data into the frequency

domain. The potential response signal E is sampled by a transient recorder.

The numeric algorithms use discrete Fourier transform methods to achieve an effective analysis. In order to minimize the errors caused by their application on single events, a weighing function has to be applied. At least, a *Zoom FFT* calculates the amplitude spectrum in the frequency domain. A similar procedure using a reference resistor was done for calibration. The quotient of both spectra finally leads to the modulus of the impedance of the unknown object.

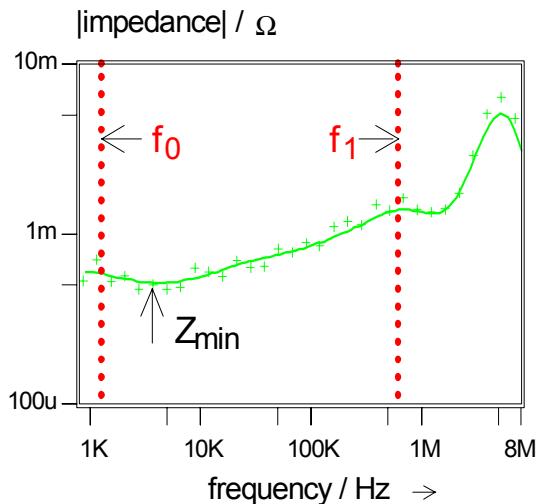


Fig. 8: Automatic evaluation of the ohmic share from the scalar impedance function.

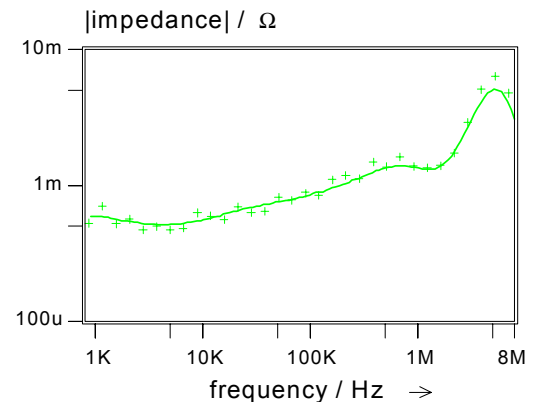
This scalar impedance spectrum can be used to evaluate the ohmic share in a simple, automated way: The user selects a reliable frequency range for analysis, which excludes the parasitic resonance at the high frequency end. The impedance minimum within this range represents the ohmic share with an acceptable accuracy of about 1 to 3%.

If you want to evaluate the response spectrum with the standard methods of the EIS, beside the impedance, the phase data will be necessary: For this calculation a relation between impedance and phase for all two pole impedance objects of minimum phase can be used. The ZHIT¹ relation allows to calculate the modulus of the impedance course from the course of the phase angle. It will also be able to perform the inverse application, if one uses the ZHIT in an iterative numeric way. This is the way, our analysis software obtains a complete spectrum.

The complex spectrum can now be analyzed in the usual way, for instance, by means of simulation and fitting of the equivalent circuit. According to our experience, the ohmic share can be determined in this way, with typically the double or triple accuracy com-

pared to the automatic minimum detection in the scalar impedance function.

Figure 10 is a sketch of the practical set-up of our high current interrupt measurement arrangement of a fuel cell. The electrochemical cell (A) is supplied by means of an electronic load (B) or another type of high power potentiostat to force the steady state load conditions. Additionally, the potentiostat acts as fast electronic switch for the current interruption.



$$\ln |Z(\eta)| \approx \text{const.} + \frac{2}{\pi} \int_{\eta_0}^{\eta} \varphi(\omega) d \ln \omega - \frac{\pi}{6} \cdot \frac{d\varphi}{d \ln \omega}(\eta)$$

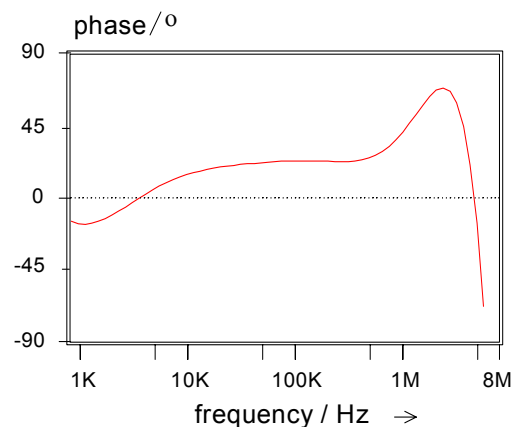


Fig. 9: Calculation of the phase angle from the impedance modulus by means of the inverse application of the ZHIT¹ transform. The ZHIT equation shows that the impedance modulus at the frequency η can be calculated from the integral of the phase angle course $\varphi(\omega)$ within limited frequency boundaries (η_0 to η). A correction term proportional to $d\varphi/d \ln \omega$ enhances the accuracy.

The potentiostat is controlled by an electrochemical workstation (D) including a high resolution transient recorder. The recorder input is connected to the potential sense lines of the cell along a so called pulse probe (C). The main task of the pulse probe is the galvanic isolation of the potential sense circuit from

¹ W. Ehm, R. Kaus, C.-A. Schiller, W. Strunz: ZHIT - a simple relation between impedance modulus and phase angle... Electrochemical Society Proceedings 2000-24, 1

the instrument in order to minimize electromagnetic interference. On the other hand, it is responsible for the protection of the instrument input by means of an energy consuming clipping circuit.

After a short 'sampling shot' during the interrupt, the instrument switches on the current again, in order to re-establish the steady state and to avoid potential damage of the cell. The pulse response is analyzed then by the software of the workstation as described before.

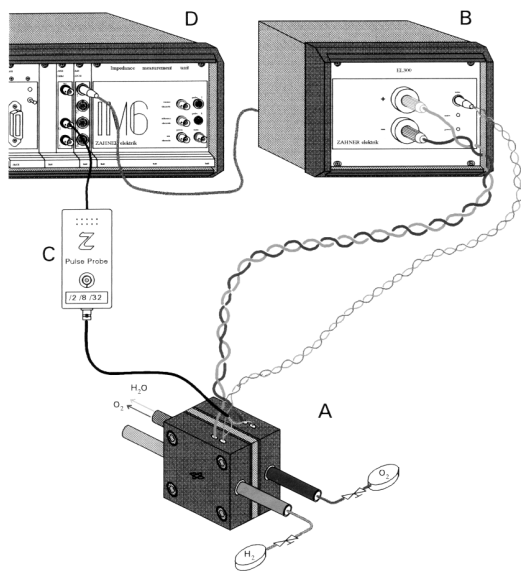


Fig. 10: Practical set-up of a high current interrupt fuel cell measurement arrangement

A lot of test experiments under controlled conditions have been done. The major experience is that, compared with the standard EIS, the HCI is much less sensitive to mutual induction artefacts. This is illustrated by the example depicted in figure 11. Here, we made test measurements at resistors using two different, intentionally non-optimized connection geometries. As you can see, the strong in-phase mutual induction of the above example leads to an inductive component which seems unrealistically high in the case of the standard EIS. The HCI method, however, leads to the almost exact value.

With the other example, which shows a strong out-of-phase mutual induction, one obtains almost the same impedance functions, which has been omitted here. Yet, the phase diagram shows paradox behaviour for the standard EIS curve: The course indicates capacitive characteristics! The phase curve of the HCI experiment shows the correct sign due to its origin from the ZHIT transform.

We also found that the HCI worked fine with power generating devices. As an example, the results of an EIS and a HCI experiment at a high temperature fuel cell are depicted in figure 12. The cell has been driven with air and humidified hydrogen and generated more than four Amperes at a potential exceeding 0.73 Volts. In both experiments the best case

wiring was used to reduce the mutual induction contribution.

The original HCI potential step response is plotted on top of figure 12. At the bottom, the transformed impedance (circles) as well as a comparative impedance measurement (rhombi) are drawn. As one can see, the methods complement each other for the different frequency ranges. In this special case, the frequency limit for the EIS experiment to get accurate information on the ohmic share is not exceeded. Therefore, both methods deliver the correct results.

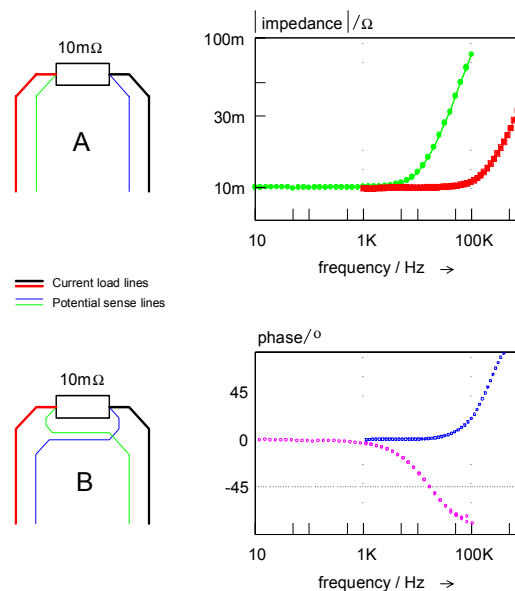


Fig. 11: Results of test measurements at reference resistors incl. mutual induction (MI) components.

A: In phase MI leads to a high inductive response in the case of EIS (full dots) whereas the HCI spectrum (squares) matches the theory.

B: Out-of-phase MI causes paradox capacitive (-) EIS phase courses (squares) while the HCI phase course shows the correct phase sign for inductance (+).

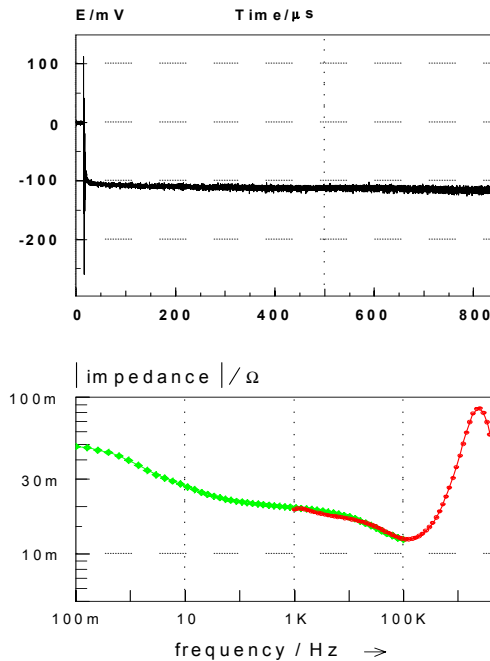


Fig. 12: High current interrupt measurement of a single solid oxide fuel cell at 866°C.
EIS: 100 mHz – 100 kHz (rhombi)
HIC: 1 kHz – 800 kHz (circles)

The last example demonstrates that the dominating error from the unavoidable mutual induction falsifies the result of standard EIS measurements at very low impedance objects. In the experiments depicted in figure 13, a HCI measurement (top) as well as a comparative EIS measurement (bottom, triangles)

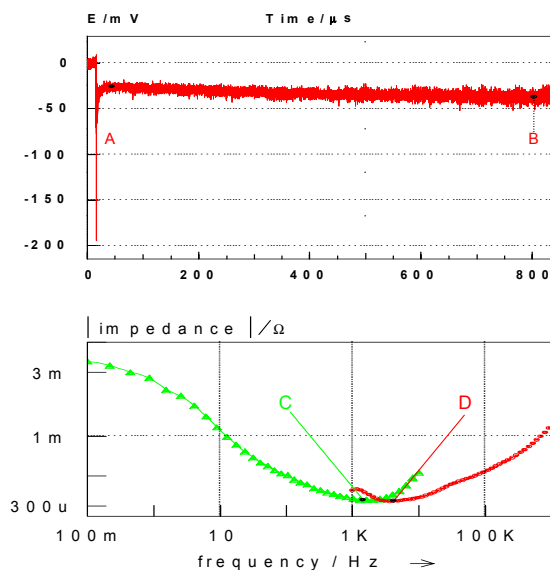


Fig. 13: High current interrupt measurement of a single PEM fuel cell at 85° C and 80 A. The resulting spectrum (C) is compared with a standard EIS (D).

on a big PEM fuel cell at a current of 80 A were performed. The shift of the increase of the impedance for the transformed HCI-data (circles) to higher frequencies indicates the smaller sensitivity of the HCI measurement against the mutual induction.

In our opinion, the missing correspondence between the EIS- and the HCI-data at the low frequency end of 1.1 KHz results from a non-linear component in the long term pulse response signal. HCI analysis has to rely on the rule of linearity. The transient changes of about -10 mV within the 0.85-millisecond-analysis-interval may be enough to violate this rule.

Conclusion

1. EIS capabilities are basically limited by mutual induction at the high-frequency low-impedance edge. This falsifies significantly the results for ohmic and inductive share.
2. The HCI capability is limited by the magnetic energy stored in the load circuit.
3. The HCI analysis can be automatically analyzed reliably by transforming the time data into the frequency domain.
4. According to our experience, HCI can extend the available frequency range about a factor of three to ten in a carefully optimized experimental set-up.
5. HCI data interpretation should not be extended to the low frequency response. The unavoidable violation of the EIS linearity rule after a certain interruption time may lead to misinterpretations.
6. Thus, an arrangement which performs both, the standard EIS and the HCI measurement within one set-up, is the best choice for the challenges of electrochemical power source device testing.

For N. American support contact:

PHIL WOLF
TEST SOLUTIONS
5665 Hwy 9 N, Ste. 103-181
Alpharetta GA 30004
USA
T: 770-410-9166
F: 443-947-0745
C: 678-231-5783
phil@test-solutions.biz
<http://www.test-solutions.biz>